RFID Tag Failure After Thermal Overstress

Emre Ozturk, Mike J. Dikkers, Kevin M. Batenburg, Cora Salm and Jurriaan Schmitz
MESA+ Institute for Nanotechnology
University of Twente
Enschede, The Netherlands
e.ozturk@utwente.nl

***Abstract*—In this work the failure modes and mechanisms are investigated of a commercially available RFID tag, when it is exposed to extreme temperatures well beyond specifications. Both erroneous functioning and malfunctioning are observed after a thermal cycle exposing the tag to an elevated temperature in the 300-550 °C range. Void formation is the dominant failure, leading to a complete malfunction of the tag. Sporadically, the RFID tag returns a wrong identification code after extreme thermal cycling. This effect is caused by relatively weak bits flipping from "1" to "0" and seems consistent with existing retention models.**

***Index Terms*—RFID, failure, thermal budget, temperature, mission profile**

I. Introduction

During their fabrication, silicon-based microchips are exposed to very high temperatures up to $\sim$1000 °C. As the fabrication progresses, the temperature excursions become progressively more modest, in particular when entering the back-end-of-line and packaging phases. Materials added in these later stages prohibit subsequent high temperature treatments [1]. As a consequence, the final packaged chip is commonly specified to operate reliably only when the temperature remains within a certain temperature range between -60 to -40 °C and 85-175 °C during its entire mission. A somewhat wider temperature range may be allowed during storage. For harsh environments where this limited temperature range cannot be guaranteed, special technologies are used, such as high-bandgap semiconductors and ceramic or wafer-level packages [2]. Further, testing for harsh environments requires a dedicated toolset [3].

RFID tags by nature can be expected to encounter a wide variety of harsh circumstances that are less likely to occur for system-integrated electronic components. This explains recent studies on the reliability of RFID tags under unconventional stress conditions such as mechanical deformation [4], immersion in water and washing [5], centrifugation, blast freezing and gamma irradiation [6].

In this article we focus on high-temperature excursions. If (short) thermal excursions beyond specifications were to be allowed, the range of applications of standard products might be larger than currently accepted. It is in this light that we investigate the robustness of a commercially available RFID tag against thermal excursions far beyond its specified use range of -40 to +85 °C. The investigations focus on device functioning *after*, not during this thermal excursion.

Lahokallio et al. [7] studied the reliability of RFID tags under thermal cycling between -40 and +125 °C with high ramp rates (85 °C/min). They showed how different parts of the tag fail depending on details in the cycling procedure. Cracks in the metallization were always the root cause for tag malfunctioning. At low ramp rates (5 °C/minute or lower) the device reliability improves [7], [8]. Taoufik et al. [9] study the effect of long-term storage at temperatures up to 160 °C accumulating to several hundred hours. A gradual reduction of the tag's response power was observed; physical analysis showed deformation of the polymer matrix and cracks in the antenna conductors.

In this work, we study newer-generation RFID tags that operate at higher frequency and consist of different materials. The tests involve shorter exposures to higher stress temperatures at modest ramp rates.

II. Experimental

The RFID tags are mass produced devices measuring approximately $3 \times 3 \times 0.7$ mm^3. They contain a silicon chip, bump-bonded to an external substrate-embedded coil, see Figure 1. Complying to the ISO15693 standard they are programmed and read out at 13.56 MHz with a smartphone held in near proximity (approximately a centimeter away). Upon readout, they should return their programmed numerical (identification) code. In this work, failure of the RFID tag is defined as a faulty returned code or no response to a readout request. Other published functionality criteria for RFID tags include the power threshold for an RFID tag to respond [7], power of the returned signal [9], or its maximum read range at given read power [10]. True loss of functionality will depend heavily on the application.

A custom-built furnace was employed for thermal cycling. The furnace offers a range of ambients including air, dry air, nitrogen and vacuum. Vacuum with $< 10^{-6}$ mbar residual pressure is maintained by a turbomolecular pump. Heating of the RFID tag is by a kanthal (FeCrAl alloy) filament; the sample lies on a sapphire substrate of which the temperature is periodically measured by a thermocouple. The setup is controlled using LabView. The temperature ramp rate in the reported experiments is 10 °C per minute; technical limitations prohibit higher ramp rates. Tags are first programmed to a unique identification code, read out, thermally cycled, and then

This work was supported by the INTERREG VA program of the European Union, project XTC-ID.

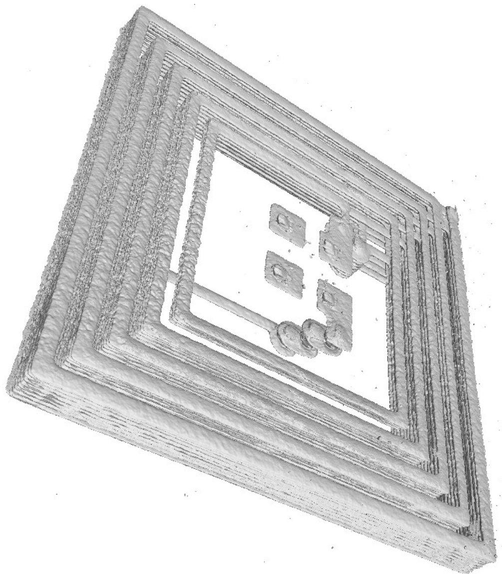

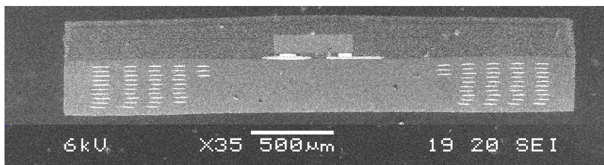

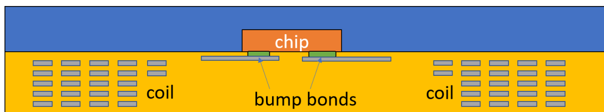

Fig. 1. Composition of the RFID tag. Top: 3D X-ray image (the centrally positioned chip is invisible in this image). Center: SEM cross-section view. Bottom: sketch indicating the main parts of the tag.

read again. Failing RFID tags were analyzed using scanning acoustic microscopy (SAM), 3D X-ray imaging, optical microscopy and scanning electron microscopy (SEM).

III. Results

A. Ramped temperature tests

In a first set of experiments, RFID tags were exposed to high-temperature excursions in vacuum with ever-increasing temperatures (with steps of 25 °C) until a no-response failure was observed. Figure 2 (inset) presents the stress-measurement cycle; a cooldown to room temperature (or at least to $\leq$ 85 °C) is necessary after each heat treatment to test the RFID tag functionality. In practice we observe that the tags under study become responsive during cooldown around 145 °C.

Four sets of thirty tags were tested, and their cumulative failure fractions are displayed in Figure 2 (main graph). The four groups were exposed to different stress times at the highest temperature (soak times t_s), while all other parameters remained the same. A first observation is that all tags survive temperature excursions up to 300 °C. This is considerably higher than previous works report for earlier-generation RFID tags with larger coils [7] - [9]. Most of these data further indicate that a longer soak time increases the probability of device failure. Therefore, the failures occur during the highest-temperature period, not during ramp-up or ramp-down.

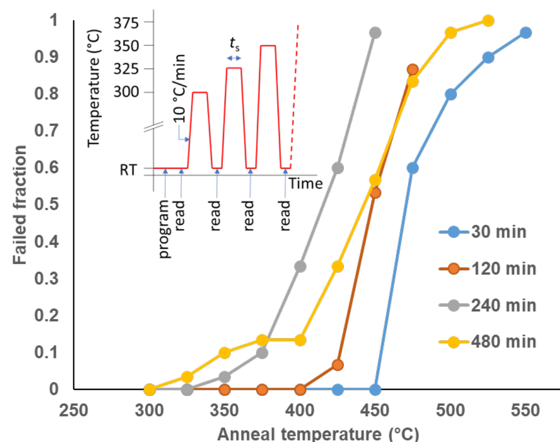

Fig. 2. Cumulative failure distributions of RFID tags exposed to ever-increasing high temperatures in vacuum for a given amount of soak time t_s. Sample size is 30 RFID tags per data set. The inset describes the measurement procedure.

The dataset with the longest soak time (480 minutes) deviates from the other three. Although the first 13% of the fails is consistently at lower temperature than the other data sets, a kink then appears in the distribution. The remainder of the samples is more robust than might be expected. The 480-minute samples have received a very long overall anneal at 300 °C. This anneal might have led to significant outgassing or material relaxation, yielding somewhat stronger devices.

Devices fail in a remarkably wide range of 325–550 °C. The tags show no visual changes after failure. SEM analysis shows cavity formation inside the device, as depicted in Figure 3. Most likely cracking creates an open-circuit somewhere in the coil. Lahokallio et al. report similar findings after repeated thermal cycling of (differently manufactured) RFID tags between -40 °C and + 125 °C [7]. They found interruptions in metal lines either in the external coil or in the microchip, depending on details in the stress procedure.

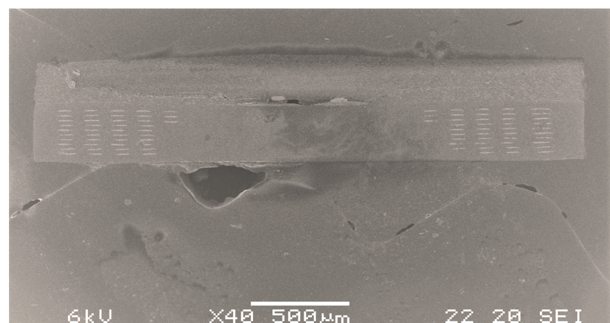

Fig. 3. SEM cross section image of a chip annealed at 400 °C in vacuum indicating cavity formation.

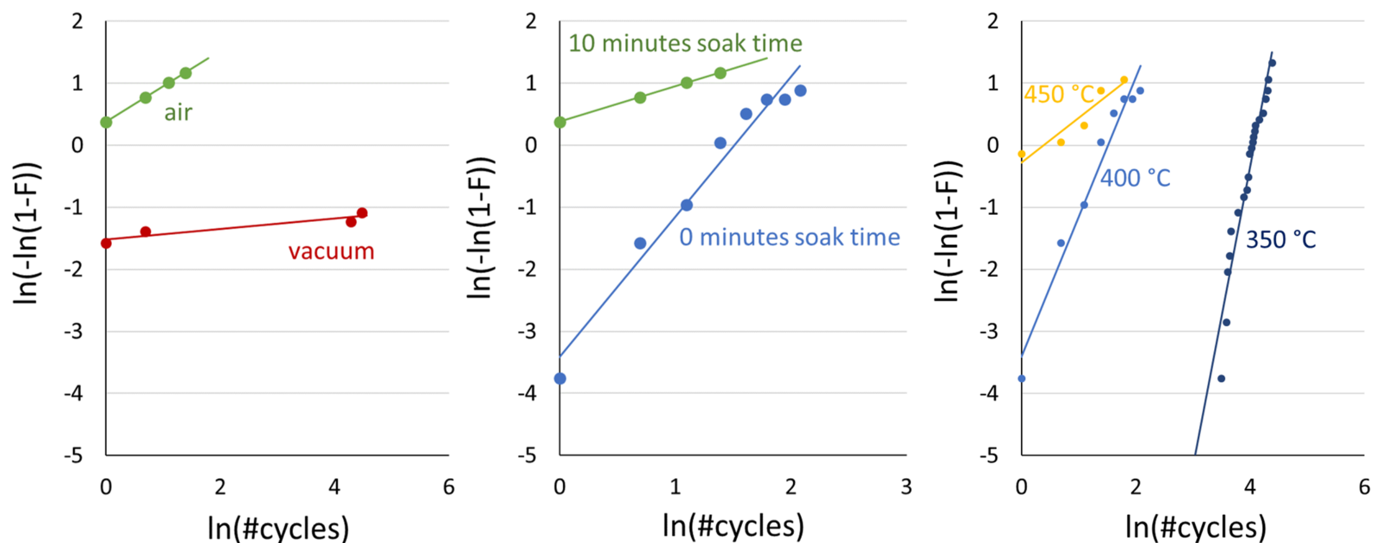

Fig. 4. Weibull distributions of RFID tag failure under thermal cycling. Left: cycling up to 400 ° C with a soak time of 10 minutes in air or in vacuum. Center: thermal cycling at various soak times with a soak temperature of 400 °C in air. Right: thermal cycling at various soak temperatures in air with a soak time of 0 minutes.

B. Thermal cycling

The same type of tags were exposed to thermal cycling tests. The temperature cycled between room temperature and a maximum (soak) temperature of 350–450 °C. The soak time was varied (0 minutes, i.e. only ramp-up and ramp-down, or 10 minutes), as well as the ambient. A comparison between annealing in air and in vacuum (Figure 4 (left)) shows strikingly different failure distributions. Cycling to 400 °C in air, the majority of the samples already fails after the first cycle. In vacuum however, most samples remain functional after a multitude of cycles; this test was aborted after 96 cycles for practical reasons. Possibly, oxygen or water vapour initiates the deterioration of the tag leading to the crack formation in case of heating in air. Moisture in particular is known to be a precursor for packaging failures [11]. Air-annealed samples show discoloration on the chip side and visible cracks. Figure 5 shows a representative cross section image of a tag after annealing in air.

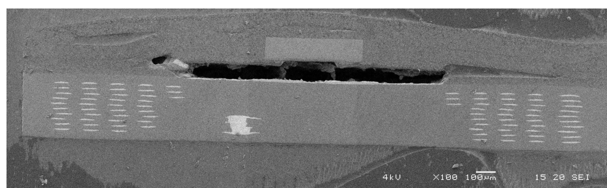

Fig. 5. SEM cross section of a failed RFID tag after thermal cycling in air, showing void formation.

The same dataset (Figure 4 (left)) shows a considerable amount of early failures, more than could be expected from the findings reported in Figure 2. This supports the idea that conditioning at somewhat lower anneal temperatures makes the RFID tag more resistant against thermal cycling; such conditioning takes place in the ramped-temperature tests, but not during thermal cycling.

As can be expected from the results presented in Figure 2, a higher temperature and a longer soak time lead to earlier failure of the chips. This is indeed confirmed by the data, as shown in Figure 4 (center and right). The monomodal Weibull distributions indicate a single failure mechanism following weakest-link statistics.

Failing RFID tags contain internal cracks. The cracks tend to propagate through a significant part of the device, going around the microchip. Scanning acoustic microscopy shows that voids concentrate around the microchip, as indicated in figure 6 and consistently observed on a multitude of samples thermally cycled in vacuum. Mismatch of thermal expansion coefficients between the materials composing the tag may lead to mechanical stress leading to shear, cracking and delamination at interfaces, as commonly reported in other works on thermal cycling of packaged microchips [11]. Functionality of the RFID tag is lost typically because the chip is disconnected from the antenna at the bumps.

Besides total loss of functionality, a different failure mode was found on the tags. After a considerable high-temperature anneal (close to the breakdown temperature) and cooldown, some tags return wrong identification codes. This occurred rarely, as depicted in Figure 7. A closer inspection showed that in those cases, bits originally programmed to “1” values had flipped to “0”. (The opposite bit flip did not occur.) No error correction is present in these RFID tags and should be implemented in the reader if this fault is to be repaired. After reprogramming of the same tag followed by additional thermal cycling, the same error is seen to occur, often at the exact same bit. Probably this bit has a relatively weak retention characteristic at elevated temperature. To the best

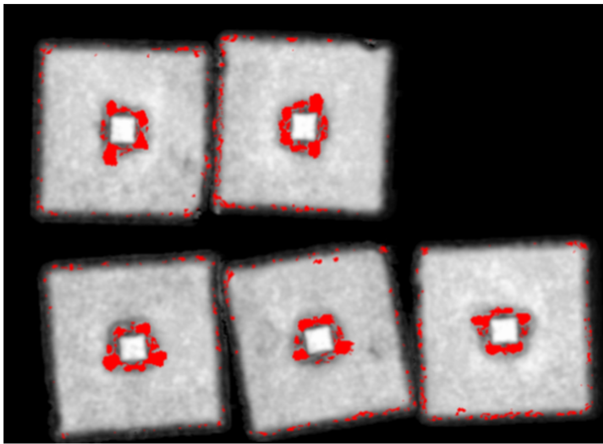

Fig. 6. Scanning acoustic microscopy top-view images of the RFID tags after thermal cycling in vacuum. The red spots indicate cavities inside the sample; the small red spots at the edges of the tag are artifacts.

of our knowledge, this failure mechanism of RFID tags after thermal annealing has not been reported earlier.

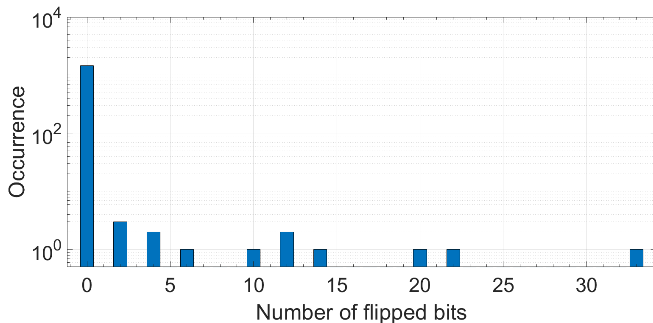

Fig. 7. Histogram of the number of wrongly returned bits in the identification code after thermal cycling of an RFID tag at 400 °C.

Given a typical specification of 10 years data retention at 25–50 °C and an activation energy for data loss due to detrapping of 1.0–1.1 eV in Flash EEPROMs [12], [13], one would in fact expect about 10^9 times faster data loss at 400 °C. This leads to the *possibility* of data loss starting already at a time scale of seconds. Here we witness limited data loss on the time scale of hours in a relatively small memory. The electrical stress on the memory is very low compared to specifications, both in terms of the number of program/erase cycles and in view of the very low number of reads (and therefore read-disturbs). Therefore a much better than worst-case retention could be expected in this test, as indeed observed (hours vs. seconds).

IV. Conclusions

RFID tags were exposed to temperatures well above their specified safe operating limits. Elevated temperatures were found to lead to two distinct failure modes. The first is related to void formation and/or cracking, leading to entirely nonresponsive tags. Such failures occur in the temperature range 325-550 °C in vacuum; in air, such damage already occurs at a lower temperature. These findings are in qualitative agreement with earlier studies conducted on earlier-generation RFID tags at lower temperatures. A second failure mode is a loss of data in the embedded EEPROM memory; bits programmed to '1' may erase which results in erroneous identification codes to be returned. Such retention errors can be expected based on conventional temperature-acceleration models for flash memories. The error tends to recur in the same bits after reprogramming, indicating the existence of relatively retention-weak cells in the memory.

Acknowledgments

We would like to thank R. A. M. Wolters, R. G. P. Sanders and S. M. Smits for fruitful discussions and technical support. M. A. Smithers is acknowledged for his assistance in deprocessing samples for SEM analysis and X. Liu for SEM photography.

References

[1] J. Schmitz, "Low temperature thin films for next-generation microelectronics", Surface & Coatings Technology, vol. 343 (2018) pp. 83–88.

[2] J. D. Cressler and H. A. Mantooth (eds.), Extreme Environment Electronics, Boca Raton, FL: CRC Press, 2013.

[3] W. C. Wilson and G. M. Atkinson, "Passive wireless sensor applications for NASA's extreme auronautical environments," IEEE Sensors Journal, vol. 14(11) (2014) pp. 3745- 3753.

[4] K. Janeczek, "Reliability analysis of UHF RFID tags under long-term mechanical cycling," Microelectronics Reliability vol. 75 (2017) pp. 96–101.

[5] M. Guibert, A. Massicart, X. Chen, H. He, J. Torres, L. Ukkonen and J. Virkki, "Washing reliability of painted, embroidered, and electro-textile wearable RFID tags," Progress in Electromagnetics Research Symposium (2017) pp. 828-831.

[6] A. Gutierrez, F. D. Nicolalde, A. Ingle, W. Hochschild, R. Veeramani, C. Hohberger and R. Davis, "High-frequency RFID tag survivability in harsh environments," 2013 IEEE Int. Conf. on RFID, pp. 58-65.

[7] S. Lahokallio, K. Saarinen-Pulli and L. Frisk, "Effects of different test profiles of temperature cycling tests on the reliability of RFID tags," Microelectronics Reliability vol. 55 (2015) pp. 93-100.

[8] S. Lahokallio, J. Kiilunen and L. Frisk, "Performance of passive RFID tags in a high temperature cycling test," 5th Electronics System-Integration Conference (ESTC 2014), art. 6962848.

[9] S. Taoufik, P. Dherbécourt, A. El Oualkadi and F. Temcamani, "Reliability and failure analysis of UHF RFID passive tags under thermal storage," IEEE Trans. Device and Materials Reliability vol. 17(3) (2017) pp. 531-538.

[10] M. Akbari, J. Virkki, L Sydänheimo and L. Ukkonen, "Toward graphene-based passive UHF RFID textile tags: a reliability study," IEEE Trans. Device and Materials Reliability vol. 16(3) (2016) pp. 429–431.

[11] E. A. Amerasekera and F. N. Najm, Failure Mechanisms in Semiconductor Devices, 2nd edition, Chichester: John Wiley & Sons, 1997.

[12] K. Lee, M. Kang, S. Seo, D. Kang, S. Kim, D. H. Li and H. Shin, "Activation energies (E_a) of failure mechanisms in advanced NAND flash cells for different generations and cycling," IEEE Trans. Electron Devices, vol. 60(3) (2013) pp. 1099-1107.

[13] JEDEC standard JESD47, Stress test driven qualification of integrated circuits, August 2018.